Developmental Cell, Volume *52*

Supplemental Information

F-Actin Interactome Reveals Vimentin as a Key Regulator of Actin Organization and Cell Mechanics in Mitosis

Murielle P. Serres, Matthias Samwer, Binh An Truong Quang, Geneviève Lavoie, Upamali Perera, Dirk Görlich, Guillaume Charras, Mark Petronczki, Philippe P. Roux, and Ewa K. Paluch

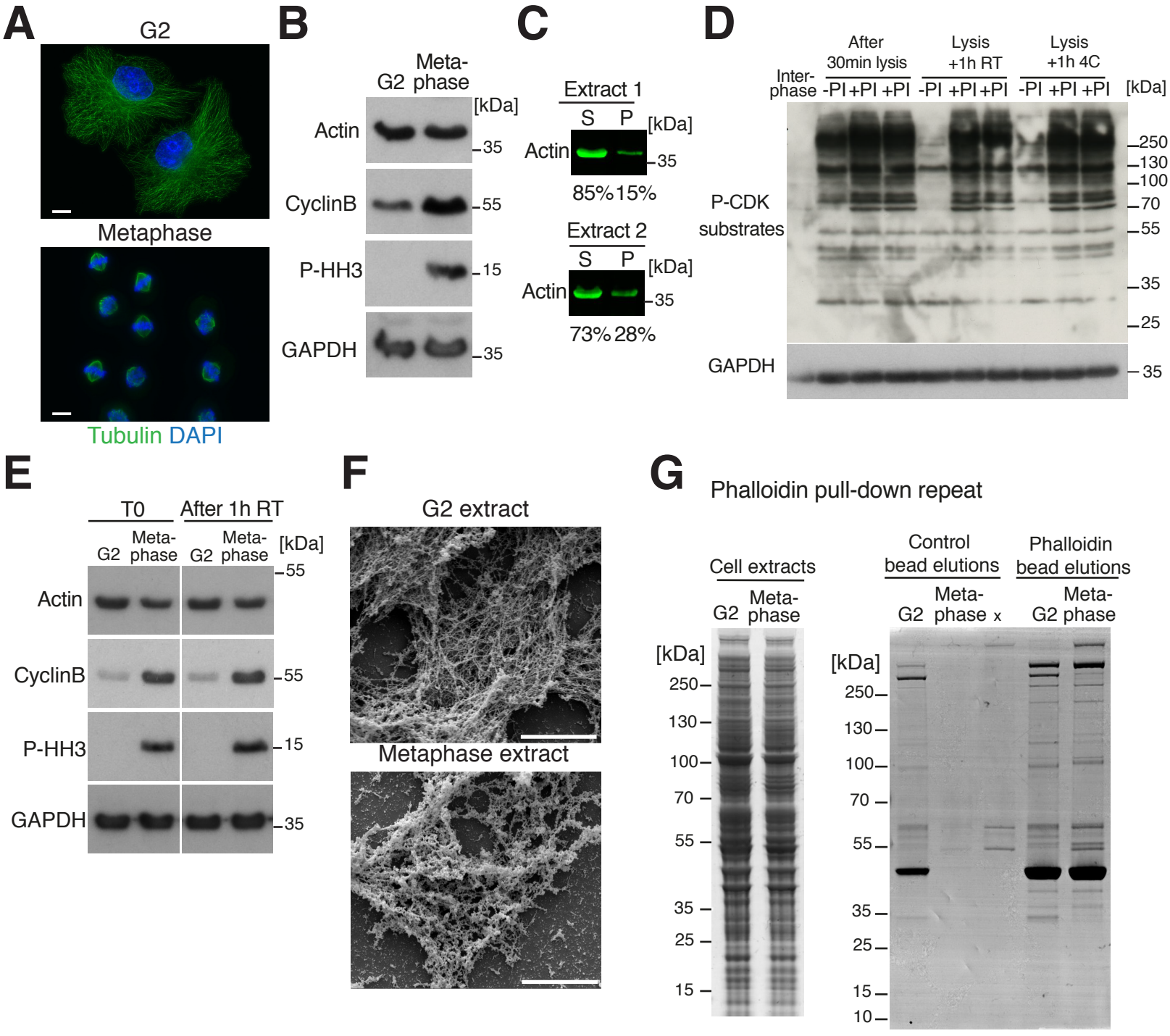

Figure S1: Additional experiments and controls for the mass spectrometry analysis of the interphase and mitotic F-actin interactomes, related to Figure 1.

(A) Representative images of microtubules (tubulin, green) and DNA (DAPI, blue) in HeLa cells synchronized in interphase (G2) and metaphase, as described in Figure 1A. Scale bars, 10 μm. **(B)** Immunoblot analysis of actin, cyclinB and phospho-Histone H3 (P-HH3) levels in synchronized cell extracts. **(C)** Fluorescent immunoblot of actin in the soluble fraction (S) versus the pellet (P) after optimization of lysis conditions. Percentages quantify the intensity of the actin bands. Extracts 1 and 2 correspond to two independent experiments. **(D)** Immunoblot analysis of phospho-CDK substrates in interphase and nocodazole-arrested mitotic cells with or without phosphatase inhibitors (PI) after different incubation conditions. RT=Room Temperature. **(E)** Immunoblot analysis of actin, cyclinB, P-HH3 levels in the synchronized cell extracts before and after 1 hour incubation at room temperature (conditions used for the phalloidin-bead pull-down). **(F)** Examples of scanning electron microscopy images of actin filaments in the synchronized cell extracts incubated with phalloidin in presence of ATP and $MgCl_2$. Scale bars, 3 μm. **(G)** Colloidal Coomassie staining of SDS-PAGE gels of synchronized cell extracts, and of the control and phalloidin bead elutions, for one of the mass spectrometry experiments (MS1); similar data corresponding to the other mass spectrometry experiment (MS2) is displayed in Figure 1D. The x marks an unrelated lane.

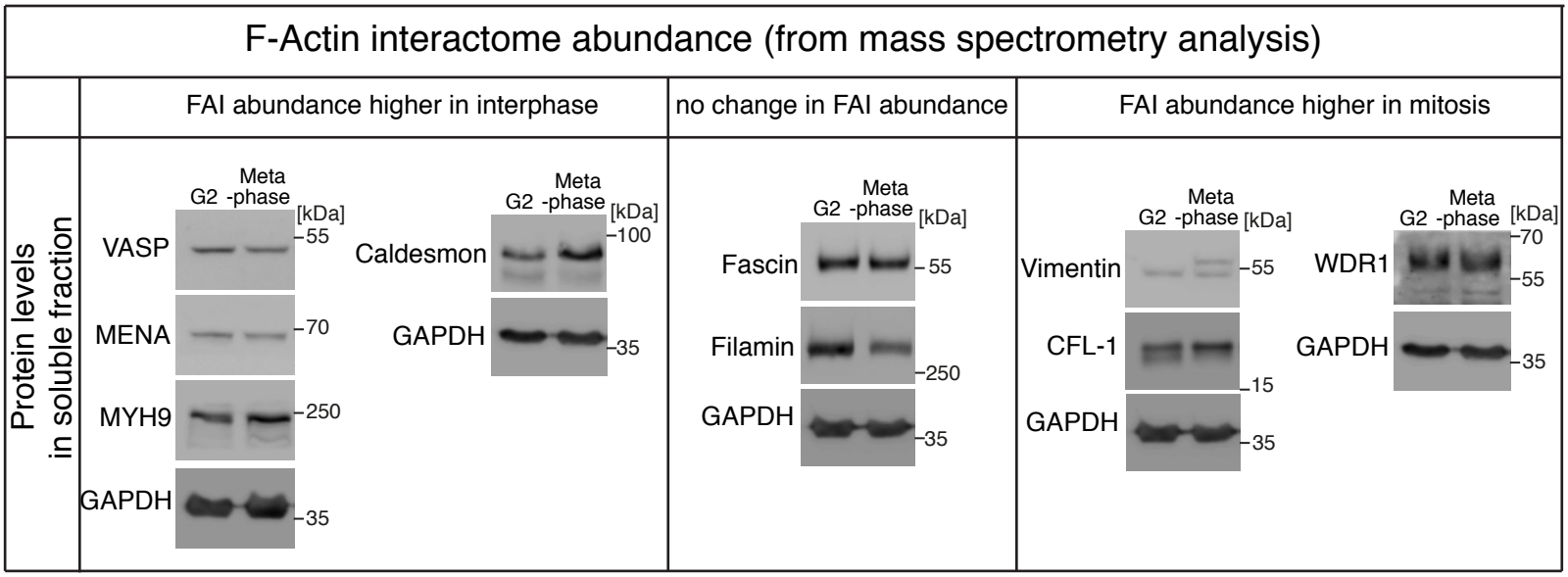

Figure S2: Changes in F-actin interactome abundance do not directly correlate with changes in protein levels in cellular fractions, related to Figure 2.

Immunoblot analysis of the levels of a subset of proteins found in the mass spectrometry analysis, in soluble fractions of cell extracts synchronized in G2 and Metaphase. GAPDH loading controls are identical for Caldesmon/WDR1 and for Fascin-Filamin/Vimentin-CFL-1, as the corresponding stainings were done on the same gel.

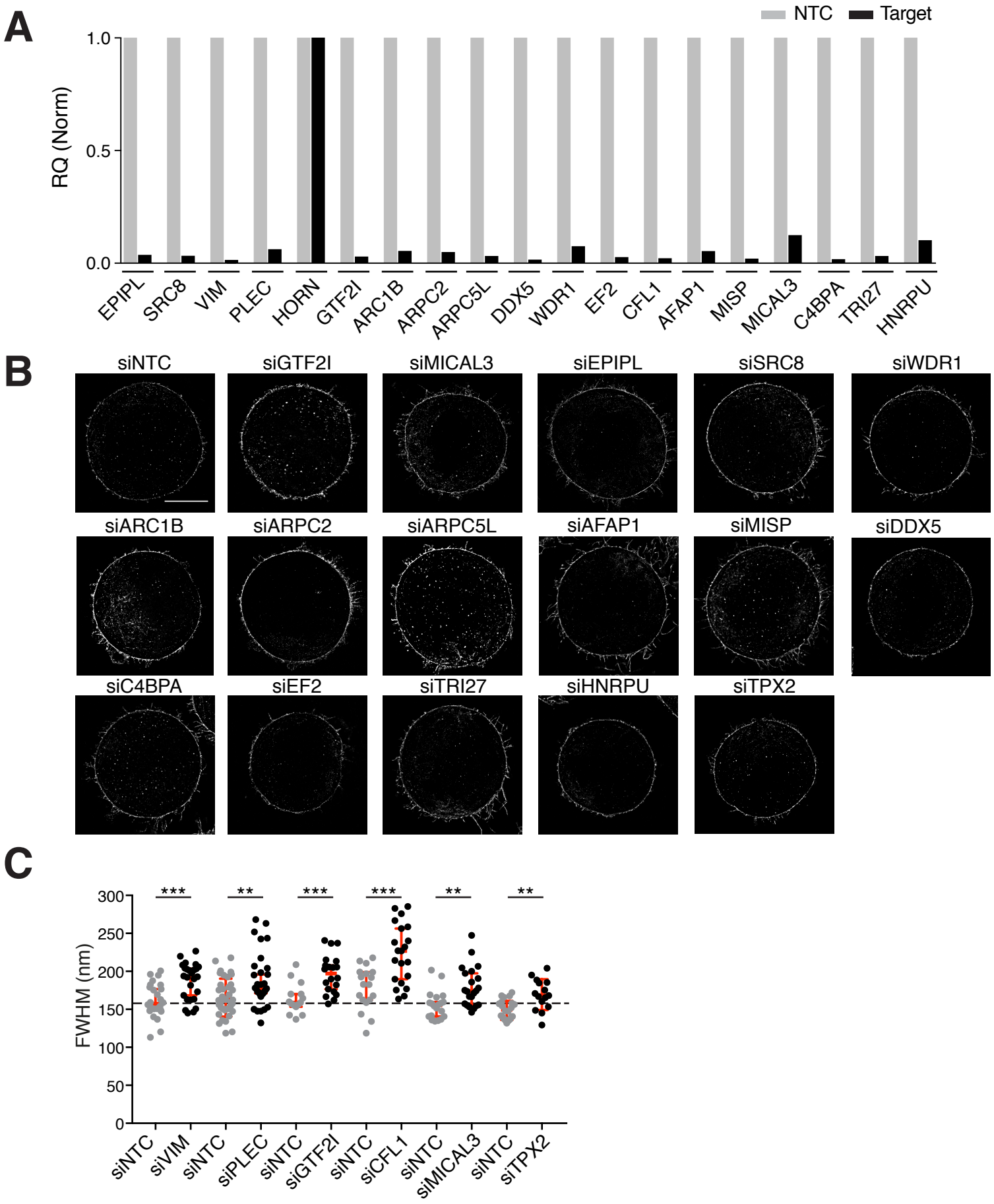

Figure S3: Additional experiments and controls on the regulation of cortical actin organization, related to Figure 3. **(A)** mRNA expression levels (RQs) in cells transfected with siRNAs against the different metaphase hits. Target RQs were normalized to the corresponding RQs of the non-targeting control (NTC) siRNAs. One protein -HORN- was excluded from further analysis, as no depletion was observed. **(B)** Examples of STORM images of the actin cortex for the different candidates tested, excluding VIM, PLEC and CFL-1, as these are shown in Figure 3C. Scale bar, 10 μm. **(C)** Non-normalized values of full width at half maximum (FWHM) of the cortical actin signal, measured for the siRNA conditions giving a significant change in Figure 3B. Unpaired Welch's t test; P-values: *** P<0.001; ** P<0.01.

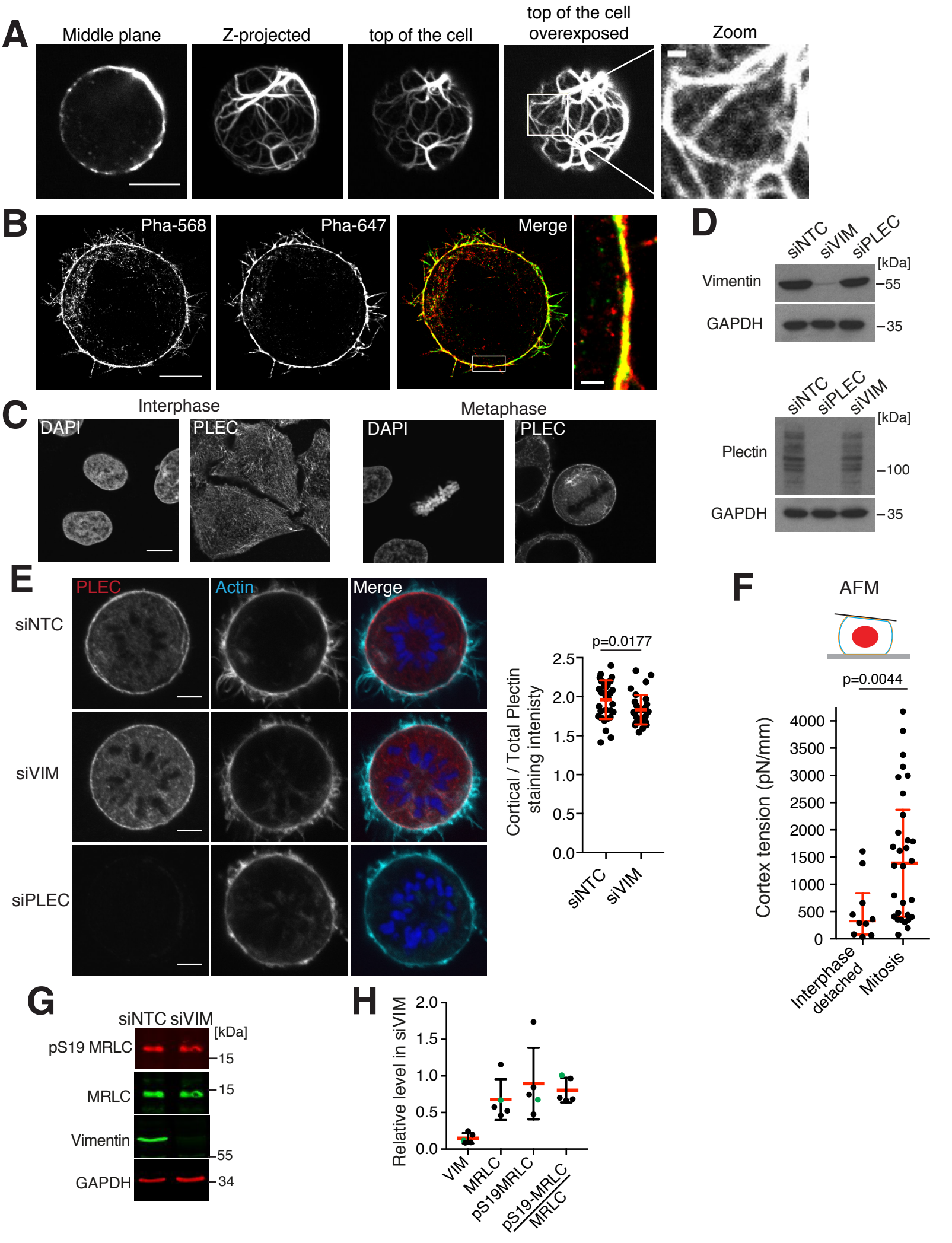
A
Middle plane
Z-projected
top of the cell
top of the cell overexposed
Zoom
B
Pha-568
Pha-647
Merge
C
Interphase
Metaphase
DAPI
PLEC
DAPI
PLEC
D
siNTC
siVIM
siPLEC
[kDa]
Vimentin
55
GAPDH
35
siNTC
siPLEC
siVIM
[kDa]
Plectin
100
GAPDH
35
E
PLEC
Actin
Merge
siNTC
siVIM
siPLEC
p=0.0177
Cortical / Total Plectin staining intensity
2.5
2.0
1.5
1.0
0.5
0.0
siNTC
siVIM
F
AFM
p=0.0044
Cortex tension (pN/mm)
4000
3500
3000
2500
2000
1500
1000
500
0
Interphase detached
Mitosis
G
siNTC siVIM
[kDa]
pS19 MRLC
15
MRLC
15
Vimentin
55
GAPDH
34
H
Relative level in siVIM
2.0
1.5
1.0
0.5
0.0
VIM
MRLC
pS19MRLC
pS19-MRLC / MRLC

Figure S4: Additional experiments and controls on the mitotic localization of vimentin to the cell cortex and on actin cortex mechanics, related to Figure 4

(A) Representative images of vimentin stainings in a mitotic HeLa cell. From left to right: Middle plane of the cell, maximum z-projection of a confocal stack across the cell, confocal image of one plane at the top of the cell and zoomed image. Scale bars, 10 μm and 3 μm **(B)** Representative 2-color STORM images of the actin cortex in mitotic cells labelled with Phalloidin-Alexa 647 and Phalloidin-Alexa 568. The peak-to-peak distance of the two actin profiles was measured as a control (Figure 4B). Scale bars, 5 μm and 1 μm. **(C)** Representative images of immunofluorescent staining of plectin in interphase and mitotic cells. DNA staining (DAPI) was used to identify cells in metaphase. Plectin formed a layer at the mitotic cortex. Scale bar, 10 μm. **(D)** Immunoblot analysis of the levels of Vimentin and Plectin in extracts of HeLa cells transfected with non-targeting control siRNA (siNTC), siRNA against plectin (siPLEC) or siRNA against vimentin (siVIM). GAPDH was used as a loading control. **(E)** Left: Representative images of plectin localization in mitotic HeLa cells transfected with non-targeting control siRNA (siNTC), siRNA against vimentin (siVIM) or siRNA against plectin (siPLEC). Scale bars, 5 μm. Right: quantification of plectin enrichment at the cell cortex. Graph: mean ± standard deviation, 3 independent experiments. siNTC: n= 32; siVIM: n= 32. Mann-Whitney test. **(F)** Cortex tension measured by Atomic Force microscopy (AFM) in cells in interphase and mitosis. Graph: median and interquartile range. Interphase detached n= 10; Mitosis n= 30; at least 2 independent experiments.Mann-Whitney test. **(G)** Representative fluorescent immunoblots of myosin regulatory light chain (MRLC) and phospho-S19 MRLC in control and vimentin-depleted cells. **(H)** Quantification of the fluorescent intensity of the vimentin, MRLC and phospho-S19 MRLC bands in vimentin-depleted cells. Intensities were normalized to corresponding GAPDH levels and the intensity in vimentin-depleted cells relative to siNTC treated cells was displayed.

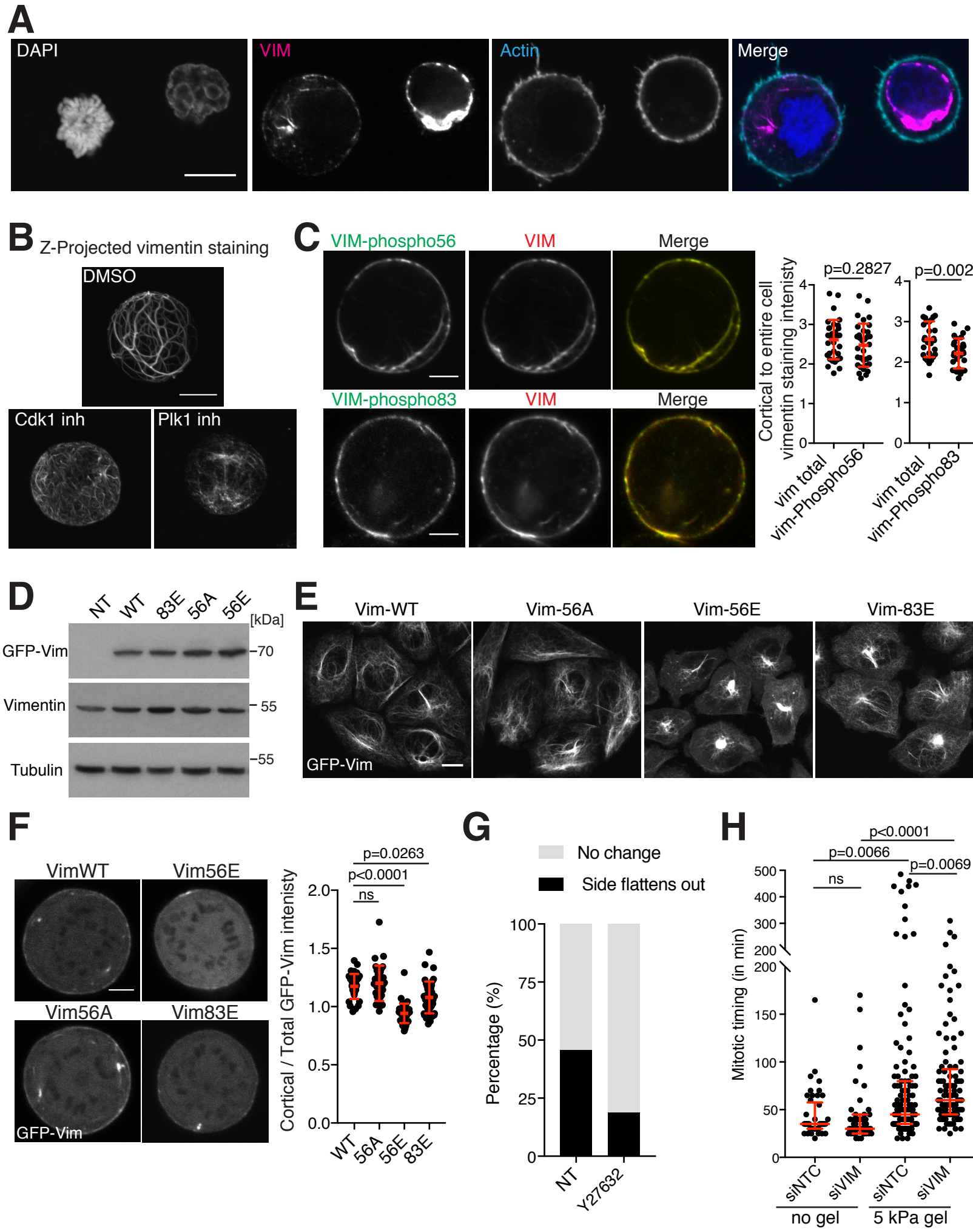
A
DAPI
VIM
Actin
Merge
B
Z-Projected vimentin staining
DMSO
Cdk1 inh
Plk1 inh
C
VIM-phospho56
VIM
Merge
VIM-phospho83
VIM
Merge
Cortical to entire cell vimentin staining intenisty
p=0.2827
p=0.0023
vim total
vim-Phospho56
vim total
vim-Phospho83
D
NT
WT
83E
56A
56E
[kDa]
GFP-Vim
70
Vimentin
55
Tubulin
55
E
Vim-WT
Vim-56A
Vim-56E
Vim-83E
GFP-Vim
F
VimWT
Vim56E
Vim56A
Vim83E
GFP-Vim
Cortical / Total GFP-Vim intenisty
p=0.0263
p<0.0001
ns
WT
56A
56E
83E
G
No change
Side flattens out
Percentage (%)
NT
Y27632
H
p<0.0001
p=0.0066
p=0.0069
ns
Mitotic timing (in min)
siNTC
siVIM
siNTC
siVIM
no gel
5 kPa gel

Figure S5: Additional experiments and controls on the effects of the sub-cortical vimentin layer on cortical actin organization in mitosis, related to Figure 5 and Figure 6.

(A) Representative images of rounded interphase (right) and mitotic (left) HeLa cells stained for vimentin and F-actin. DAPI staining was used to identify interphase cells. Scale bar, 10 μm **(B)** Representative maximum z-projections of confocal stacks across mitotic HeLa cells treated with DMSO, CDK1 inhibitor or PLK1 inhibitor and stained for total vimentin (see Video S3 for 3D visualizations). Scale bar, 10 μm **(C)** Left: Representative images of mitotic HeLa cells immunostained for phospho-56 or phospho-83 vimentin and total vimentin (VIM). Right: quantification of phospho-56 or phospho-83 vimentin enrichment at the cell cortex. Graph: mean ± standard deviation, 3 independent experiments. Vimentin total and phospho-56: n= 33; Vimentin total and phospho-83: n= 28. Unpaired t-test. Scale bars, 5 μm. **(D)** Immunoblot analysis of the levels of GFP-Vimentin in extracts of HeLa cells stably expressing different GFP-Vimentin mutants. NT: Non-transfected. **(E)** Representative images of interphase HeLa cells stably expressing different GFP-vimentins (WT and mutants as indicated). Scale bar, 10 μm. **(F)** Left: Representative images of GFP-vimentin (WT and mutants as indicated) localization in mitotic HeLa cells stably expressing GFP-vimentin WT or mutants. Right: quantification of GFP enrichment at the cell cortex. Graph: mean ± standard deviation, 3 independent experiments. WT: n= 31; 56A: n= 31; 56E: n= 33; 83E n= 29. Kruskal-Wallis test; ns=non-significant. Scale bar, 5 μm. **(G)** Effects of the ROCK inhibitor Y27632 in laser ablation experiments in HeLa cells expressing GFP-Vimentin-WT. The treatment with ROCK inhibitor abolished the occurrence of blebs (corresponding to 5 cells out of 27 in control condition compared to 1 cell out of 60 in Y27632 treated cells) confirming it effectively reduces cortex contractility, and strongly reduced the proportion of cells displaying surface flattening upon ablation; 18% of Y27632-treated cells still displayed visible surface flattening (vs. 45.5% in control cells), possibly because Y27632 treatment reduces but does not entirely abolish cortical tension (Tinevez et al PNAS 2009). **(H)** Mitotic timing (from nuclear envelope break down to anaphase onset) in control and vimentin-depleted cells unconfined (no gel), and confined under 5 kPa gels. Graph: median and interquartile range. No gel: siNTC: n= 46; siVIM: n= 46; 5 KPa gel: siNTC: n= 122; siVIM: n= 102; at least 3 independent experiments. ANOVA non-parametric Kruskal-Wallis test; ns, non-significant.

Protein name	GENE ID	Forward primer	Reverse primer	siRNA Pool Catalog Number	siRNA Sequences
ACTB	60	attggcaatgagcggttc	tgaaggtagtttcgtggatgc		
GAPDH	2597	agccacatcgctcagacac	gcccaatacgaccaaatcc		
VIME	7431	aaagtgtggctgccaagaac	agcctcagagaggtcagcaa	M-003551-02	UGAAGAAACUCCACGAAGA ; GCAGAAGAAUGGUACAAAU ; UGAAGUGGAUGCCCUUAAA ; AACUAGAGAUGGACAGGUU
TRI27	5987	gcctgatcgctcagctagaa	caatgtgtccccaatgtcc	M-006552-01	GAGCAGGGCUGAAAGAAUC ; UAAGAGAGGCUCAGUUAUA GCUGAACUCUUGAGCCUAA ; GAAGAUUGUUUGGGAGUUU
ARC1B	10095	ggcgctgaccttcatcac	gcgtcataggtgaacagcac	M-012082-01	GAGAAUGACUGGUGGGUUU ; GAGAGUAACCGUAUUGUGA UAGACUCGCUGCACAAGAA ; GCACAGACCGCAACGCCUA
GTF2I	2969	ttgaggactatttctgcttttgc	cccctgcactaccacagc	M-013638-00	CAAGUGGGCAAUCGAAUUA ; GAAGGUGCCGUUCGCGUUA GCAAAUCGGAUGAGUGUAG ; CGAAGUCCCUCAUGGUAUG
ARPC2	10109	gccccacaggtcctcttta	tgacgagggaacagcaca	M-012081-00	GCAUCAAGCUGGCAUGUUG; GUACGGGAGUUUCUUGGUA GGAGAGAACAGGGCAGUUA; CCAUGUAUGUUGAGUCUAA
CS021	126353	tgtgcccatcgaggagtc	gagacctctgggcttactgc	M-018420-00	GAAAGAAGGAGCAAUGGUA ; GAUGAGGGUUGGCAGGUUU CGACCCAGCUCCAGAAGUG ; GCAGUUACUCGGUGUCUGA
COF1	1072	gtgccctctccttttcgttt	ttgaacaccttgatgacaccat	M-012707-00	UGACAGGGAUCAAGCAUGA ; GCGGUGCUCUUCUGCCUGA GUCAAGAUGCUGCCAGAUA ; GCUAUGCCCUCUAUGAUGC
MICA3	57553	tttgctggacaaaggagtga	cctccctggcatagctga	M-024432-02	CCGUACAGCCAUCGACUUA ; UUUAUAUGAUACUGGCGAA GAGGAUGGACGUUGCCGUU ; CGCACAGUCCAUCGGCAUA
TPX2	22974	tgaggcagccatatcaagaa	ccttctgagcagaaagcctaag	M-010571-00	UGACAACACUUACUACAAA; GGACGAACCGGUAGUGAUA AGACAAAGAACGUCAGUUA ; GAACUUUACAUCUGAACUA
HNRPU	3192	gaaacaatcgtggctacaaaaa	gcttctgaccccagaattga	M-013501-01	GGAAAGACCUACCAGAACA; GUAGAACUCUCGUAUGCUA GAACAGAAAGGCGGAGAUA ; CGUAUUGGCUGGUCACUAA
SRC8	2017	tcggaaccggaagtagagc	aggcattggggactgattc	M-010508-00	GAACAAGACCGAAUGGAUA ; GAAUAUCAGUCGAAACUUU GGACAGAGUUGAUCAGUCU ; ACAGAGAGAUUACUCCAAA
WDR1	9948	agaaacaaccccagcaagc	cgtggctcccagagtaaatg	M-011984-02	GGAAAGUGCGUCAUCCUAA ; GGUGGGAUUUACGCAAUUA GCGGCAAGUCCUACAUUUA ; UUGUCAACUGUGUGCGAUU
EF2	1938	gagacggtcagtgaagagtcg	tacagccggttgtgcttgt	M-007245-02	CAAAGGCCCUCUUAUGAUG ; GCUGCGAGCUCCUGUACGA ACAACCGGCUGUACAUGAA ; GGACAUCGAUAAAGGCGAG
C4BPA	722	aaatgaccttgatcgctgct	ataaagtgggtggaggacca	M-007817-01	CCAAGGAUGUGAGGCGUUA ; CAAAUAGAAUUCAGCUGUU CUACAGAGAGACAGCGCAA ; GCUACAUUCUGGUCGGACA
DDX5	1655	cagactggatctgggaaaacat	gtgccagcaccaaacaaa	M-003774-01	CACAAGAGGUGGAAACAUA ; GUGAUGAGCUUACCAGAAA GCAAAUGUCAUGGAUGUUA ; GGAUGUGUGUCAUGACGUA
PLEC	5339	ctcggagctggagctgac	accaggctgatggtcttga	M-003945-03	GAGCUAAUGUGGCUGAAUG ; GCACUGCGUAGGAAAUACA CGGAAUACUUCACGGCAGA ; GUGCCAGAGGUUUGCGAAA
AFAP1	60312	ccgtccagagcaaggaac	ggccactacaaccactgtagg	M-013084-01	CGGAAUACAUCACAUCAAA ; UUACGUACAUCCCGAAAGA GCUCUUAUGAGUCGUAUGA ; GGUGCCGAGUGAAAGAUAA
ARPC5	81873	cagaaaatagcagcgcagtg	gcctagtcctcctactgctaagg	M-014690-00	GCGUUGACUUGUUAAUGAA ; UCACAAACUUCAAGAGCAG UCGACGAAUUUGACGAGAA ; CUUAGCAGUAGGAGGACUA
EPIPL	83481	ggcaggacagaggtggac	ggccactcatcacacacg	M-032712-00	GGAAAGAAACCUACGUGAA ; CAGUGGAGGACGCGGUUAA GAAACGGGACGGAGCACGA; CCGAAUACGUUGGCGCUGA
HORN	388697	catggcagtcctctggttg	cctagagccgtgttgttcgt	M-027450-01	GCAACAUGGUUCUACAUCA; GAACGACACGGAUCUAGCU CGACAUGGGUCCGGUUUGG; UAGUAGCACUUCACCCUAU

Table S2: Primers and siRNA used in this study, related to Figures 3 and S3.